MODERN X-RAY SPECTRAL METHODS IN THE STUDY OF THE ELECTRONIC STRUCTURE OF ACTINIDE COMPOUNDS: URANIUM OXIDE UO_2 AS AN EXAMPLE

by

Yury A. TETERIN, Anton Yu. TETERIN

Received on June 25, 2004; accepted on November 8, 2004

Fine X-ray photoelectron spectral (XPS) structure of uranium dioxide UO_2 in the binding energy (BE) range 0-~40 eV was associated mostly with the electrons of the outer (OVMO) (0-15 eV BE) and inner (IVMO) (15-40 eV BE) valence molecular orbitals formed from the incompletely U5f,6d,7s and O2p and completely filled U6p and O2s shells of neighboring uranium and oxygen ions. It agrees with the relativistic calculation results of the electronic structure for the $UO_8^{12-}(O_h)$ cluster reflecting uranium close environment in UO_2, and was confirmed by the X-ray (conversion electron, non-resonance and resonance $O_{4,5}$(U) emission, near $O_{4,5}$(U) edge absorption, resonance photoelectron, Auger) spectroscopy data. The fine OVMO and IVMO related XPS structure was established to yield conclusions on the degree of participation of the U6p,5f electrons in the chemical bond, uranium close environment structure and interatomic distances in oxides. Total contribution of the IVMO electrons to the covalent part of the chemical bond can be comparable with that of the OVMO electrons. It has to be noted that the IVMO formation can take place in compounds of any elements from the periodic table. It is a novel scientific fact in solid-state chemistry and physics.

Key words: X-ray photoelectron spectroscopy, conversion electron spectroscopy, X-ray emission spectra, resonant X-ray emission spectra, X-ray absorption spectroscopy, resonant X-ray photoelectron spectroscopy

INTRODUCTION

While studying uranium compounds with the XPS method it has been traditionally suggested that only low binding energy incompletely filled electronic shells (0-~15 eV BE) participate in the chemical bond formation. To a certain degree, it is a consequence of the widespread use of visible and ultraviolet excitation sources in atomic and molecular spectroscopy. Hence, X-ray emission studies were also focused on these electron energies, neglecting the fact that quantum mechanics does not forbid the participation of relatively deep (~15-~50 eV BE) filled electronic shells in the IVMO formation and that their influence on the overall interatomic binding in various compounds may not be negligible when compared to the contribution of OVMO (0-~15 eV BE). However, it has been shown during the last few years that under certain conditions the IVMOs can be formed in compounds composed of almost any element of the periodic table [1–5]. These findings are extremely important in solid-state physics and chemistry.

This work considers new data on the chemical bond nature using UO_2 as an example. These data were obtained using modern X-ray spectral methods, such as: X-ray photoelectron, conversion electron, non-resonant, and resonant X-ray $O_{4,5}$(U) emission, near $O_{4,5}$(U) edge absorption, resonant photoelectron and oxygen Auger spectroscopy; as well as the relativistic electronic structure calculation for the $UO_8^{12-}(O_h)$ cluster reflecting an uranium close environment in UO_2. Since IVMO formation is general, the data for uranium dioxide can be used for the study of the chemical bond nature

Scientific paper
UDC: 539.194...164
BIBLID: 1451-3994, *19* (2004), 2, pp. 3-14

Authors' address:
Russian Research Center "Kurchatov Institute"
1, Kurchatov square, Moscow 123182, Russia

E-mail address of corresponding author:
teterin@ignph.kiae.ru (Y. A. Teterin)

not only in actinide compounds, but also in compounds of other elements.

EXPERIMENTAL

X-ray photoelectron spectroscopy (XPS) and OKLL Auger spectra of solid UO_2 [6] were measured at room temperature using an electrostatic spectrometer (Hewlett-Packard, HP 5950A) employing a monochromatic $AlK_{\alpha 1,2}$ ($h\nu$ = 1486.6 eV) radiation in a vacuum of 1.3 10^{-7} Pa. The device resolution measured as full width on the half-maximum (FWHM) of the $Au4f_{7/2}$ line on the standard rectangular golden plate was 0.8 eV. The binding energies [eV] were measured relative to the binding energy of the C1s electrons from hydrocarbons absorbed on the sample surface which equals to 285.0 eV. The FWHM were measured relative to the width of the C1s line of hydrocarbons (1.3 eV). The error in determination of electron binding energies and the line widths did not exceeded 0.1 eV and that of the relative line intensities was less than 10%.

The conversion electron spectra (CES) were measured with the same spectrometer using an extra accelerating electronic system and widened up to ~2500 eV energy range without any significant changes of device parameters. The sample preparation has been described in [7].

X-ray $O_{4,5}$(U) emission spectra (XES) of UO_2 were measured with a spectrometer RSM-500 with an energy resolution of 0.3 eV. Spectra were recorded at the X-ray tube voltage of 1 kV (15 mA) and 3 kV (5 mA). The samples were settled on a silver plate which served as an X-ray tube anode [8].

Resonant X-ray $O_{4,5}$(U) emission spectra (RXES) were collected at the undulator Beamline 7.0.1 of the Advanced Light Source (ALS) at the Lawrence Berkeley National Laboratory [9]. Experiments were done in the XES branchline chamber at approximately 6.7 10^{-4} Pa. The RXES spectra were measured with the incident beam at ~75° to the substrate surface. The beam size was less than 1 mm^2. The grazing-incidence fluorescence grating spectrometer with a two-dimensional position sensitive detector was used to measure the RXES spectra. The energies were calibrated using the elastic scattering features. The total electron yield spectra were measured in current mode with the incident beam perpendicular to the substrate surface.

Resonant photoelectron (RXPES) and total electron yield spectra of UO_2 were measured at the Russian-German Beamline BESSY II in Berlin. A thin UO_2 film on metallic uranium foil was used as a sample [10].

The self-consisting field relativistic X_α discrete variation (SCF X_α-DV) calculation results for the UO_8^{12-} (O_h) cluster at $R_{U\text{-}O}$ = 2.37 10^{-10} m [11] were used for the interpretation of the XPS and other spectral data.

RESULTS AND DISCUSSION

X-ray photoelectron spectroscopy (XPS). The low binding energy (0-40 eV) XPS from UO_2 can be conditionally subdivided into two energy ranges (fig. 1). The first one, 0-13 eV, shows the structure attributed to the OVMOs built mostly from the incompletely filled outer U5f,6d,7s and O2p AOs (tab. 1). The second one, 13-40 eV, shows the IVMO related fine structure. These IVMOs are built mostly from the completely filled inner valence U6p and O2s AOs. The OVMO XPS structure has typical features and can be subdivided into the four components. The IVMO spectral range exhibits pronounced peaks and can be subdivided into six components (fig. 1). Taking into account the MO compositions and photoionization cross-sections (tab. 1, [12]) the theoretical spectral intensities for

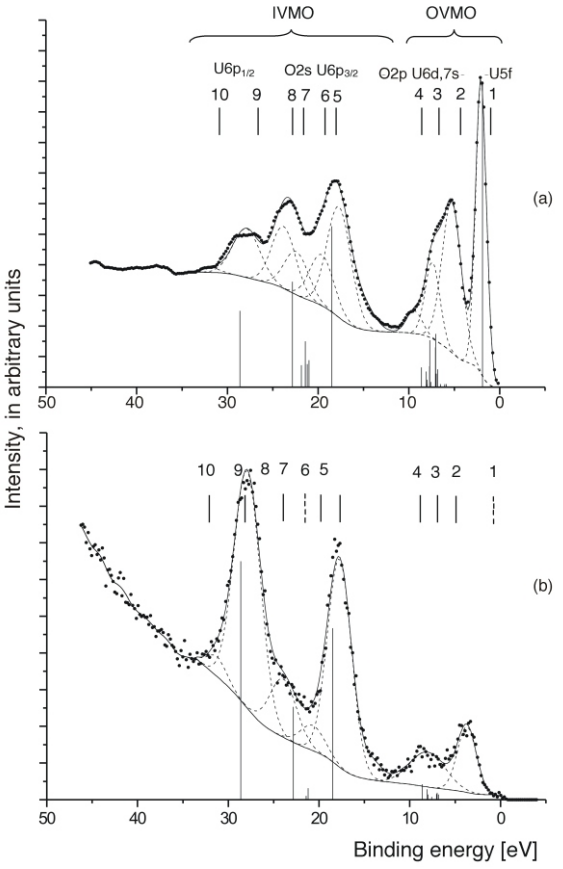

Figure 1. XPS (a) and CES (b) from UO_2. The corresponding theoretical spectra are given bellow the experimental spectra as vertical bars. The shape of subtracted background and spectra decomposition are shown. The experimental spectral intensities are given in arbitrary units, the theoretical intensities are normalized in %.

Table 1. MO composition and energies E_0(a) [eV] for the $UO_8^{12-}(O_h)$ at R_{U-O} = 2.37 (RX_α-DVM), photoionization cross-sections σ_i [12] and conversion one-electron partial probabilities α_i [15]

	MO	Q	$-E_0$(a), [eV]	MO composition												
				U										O		
				6s	$6p_{1/2}$	$6p_{3/2}$	$6d_{3/2}$	$6d_{5/2}$	7s	$5f_{5/2}$	$5f_{7/2}$	$7p_{1/2}$	$7p_{3/2}$	2s	$2p_{1/2}$	$2p_{3/2}$
				$_i$ 1.14 $_i$ 0.07	0.89 49.38	1.29 23.55	0.61 6.55	0.55 7.71	0.12 0.01	3.67 0.07	3.48 0.04	0.07 8.23	0.10 4.39	0.96	0.07	0.07
OVMO	8 $_7^+$	0	–6.09					0.84						0.04	0.10	0.02
	14 $_8^+$	0	–5.85				0.42	0.41						0.04	0.02	0.11
	11 $_6^+$	0	–4.18						0.90					0.05	0.02	0.03
	13 $_8^+$	0	–2.33				0.39	0.47							0.04	0.10
	16 $^-$	0	–1.78							0.01	0.01		0.91	0.03		0.04
	$^-$	0	–1.52									0.92		0.03	0.04	0.01
	$^-$	0	–1.50							0.12	0.75			0.01	0.06	0.06
	$^-$	0	–0.77								0.94				0.06	
	$^-$	0	–0.73								0.81		0.15	0.01	0.01	0.02
	$^-$	0	–0.08							0.78	0.16				0.01	0.05
	14 $_8^{(-b)}$	2	0.00							0.92			0.01			0.07
	13 $_8^-$	4	3.97												0.32	0.68
	12 $_8^+$	4	4.14												0.16	0.84
	10 $_6^+$	2	4.19												0.66	0.34
	7 $_7^+$	2	4.60												0.13	0.87
	11 $_8^+$	4	4.62												0.43	0.57
	10 $_6^-$	2	4.93		0.01						0.05	0.05			0.89	
	11 $_8^-$	4	5.08			0.02					0.01		0.02		0.21	0.74
	12 $_8^-$	4	5.16			0.02				0.06	0.01		0.05		0.03	0.83
	6 $_7^-$	2	5.19							0.06	0.06				0.30	0.58
	9 $_6^-$	2	5.69		0.01						0.01	0.01				0.97
	10 $_8^-$	4	5.81							0.03	0.04				0.18	0.75
	5 $_7^-$	2	5.83							0.04	0.02				0.63	0.31
	6 $_7^+$	2	6.10					0.11						0.02	0.76	0.11
	9 $_6^+$	2	6.16	0.01					0.04					0.02	0.32	0.61
	10 $_8^+$	4	6.19				0.07	0.05						0.02	0.08	78.0
	9 $_8^+$	4	6.72				0.08	0.10							0.25	0.57
IVMO	9 $_8^-$	4	16.60			0.63							0.01	0.33	0.01	0.02
	4 $_7^-$	2	19.11							0.01	0.01			0.98		
	8 $_6^-$	2	19.30		0.04							0.03		0.93		
	5 $_7^+$	2	19.51					0.06						0.94		
	8 $_8^+$	4	19.51				0.03	0.02						0.95		
	8 $_6^+$	2	19.94	0.01					0.06					0.93		
	8 $_8^-$	4	20.93			0.34							0.01	0.63	0.01	0.01
	7 $_6^-$	2	26.73		0.95									0.04		0.01
	7 $_6^+$	2	43.27	0.99										0.01		

(a) Calculated energies are shifted down toward the negative values by 7.5 [eV] of absolute scale
(b) Upper filled orbital 14 $_8^-$ (2 electrons), filling number for n $_6^\pm$ and n $_7^\pm$ MO is 2, for n $_8^\pm$ – 4 electrons

some energy ranges were determined (tab. 2, fig. 1). Despite the approximation imperfections, one can see a good qualitative agreement between theoretical and experimental data. For example, the corresponding theoretical and experimental FWHMs and relative intensities of the outer and inner valence bands are comparable. A satisfactory agreement also was achieved between the theoretical and experimental binding energies for some electronic orbitals (tab. 2). The worst agreement was reached for the middle (4 $_7^-$ - 8 $_8^-$) IVMO region. The relativistic calculation enabled the interpretation of the XPS fine structure in the whole range 0–40 eV.

Thus, the peak at 1.9 eV BE is attributed to the U5f electrons, and the outer valence band – to the outer valence U5f,6d,7s,7p and O2p AOs and to a lesser degree – to the U6p AO. Practically, such experimental evidence establishes the fact that the U5f electrons can participate in the chemical bond without loosing their f-nature. The experimental intensity ratios OVMO/IVMO with (and without) taking into account the U5f line intensity are 0.98 (0.56), which slightly differs from the corresponding theoretical values 1.16 (0.53) (tab. 2). The 15% in the parentheses is due to the U5f electrons. Since the U5f AO practically does not participate in the IVMO formation, one of the reasons for the difference between these data can be the increase of the oxygen coefficient x in UO_{2+x}, which leads to the decrease of the experimental U5f intensity. Associating, for example, the OVMO intensity only with the $U6d^17s^25f^3$ and $2O2p^4$ electrons, and the IVMO intensity – with the $U6p^6$ and $2O2s^2$ electrons in uranium dioxide, one can get a corresponding theoretical OVMO/IVMIO ratio of 1.15, which is somewhat higher than the corresponding

Table 2. XPS and CES parameters for the $UO_8^{12-}(O_h)$ cluster at $R_{U\text{-}O}$ = 2.37 nm (RX_α-DVM), and the U6p electronic state density ρ_i (e^-) in UO_2

MO	$-E$[a], [eV]	XPS Energy[b], [eV]	XPS Intensity [%]		CES Energy[b], [eV]	CES Intensity [%]		Experimental U6p electronic state density ρ_i [e^- units]	
		Experiment	Theory	Experiment	Experiment	Theory	Experiment	$U6p_{3/2}$	$U6p_{1/2}$
$14\ 8^{-}$[c]	1.90	1.9 (1.4)	29.3	21.4		0.1			
$13\ 8^{-}$	5.87	5.3 (2.5)	0.3	19.1	3.7 (2.5)		7.5	0.5	0.1
$12\ 8^{+}$	6.04		0.3						
$10\ 6^{+}$	6.09		0.1						
$7\ 7^{+}$	6.50		0.1						
$11\ 8^{+}$	6.52		0.3						
$10\ 6^{-}$	6.83		1.7			0.9			
$11\ 8^{-}$	6.98		1.3			1.1			
$12\ 8^{-}$	7.06		5.1			0.9			
$6\ 7^{-}$	7.09		3.8						
$9\ 6^{-}$	7.59	7.4 (1.9)	0.5	7.4		0.5			
$10\ 8^{-}$	7.71		4.5						
$5\ 7^{-}$	7.73		2.0						
$6\ 7^{+}$	8.00		0.7		8.0 (4.5)	0.8	7.3		
$9\ 6^{+}$	8.06		0.3						
$10\ 8^{+}$	8.09		1.5			1.7			
$9\ 8^{+}$	8.62	9.4 (1.6)	1.9	1.7		2.5			
I_i[d]			53.7	49.6		8.5	14.8	0.5	0.1
$9\ 8^{-}$	18.50	17.7 (3.1)	15.3	16.9	17.8 (3.1)	29.2	32.3	2.7	
$4\ 7^{-}$	21.01	19.6 (3.0)	2.6	8.1					
$8\ 6^{-}$	21.20		2.2		20.7 (3.1)	2.2	3.6		0.2
$5\ 7^{+}$	21.41		2.2			0.5			
$8\ 8^{+}$	21.41	22.4 (3.2)	4.4	6.9		0.7			
$8\ 6+$	21.84		2.1						
$8\ 8^{-}$	22.83	23.8 (3.3)	10.1	9.9	23.9 (3.4)	15.8	9.3	0.8	
$7\ 6^{-}$	28.63	27.9 (3.5)	7.3	7.3	27.9 (3.4)	43.1	37.7		1.6
Sat		31.1 (2.3)		1.3	31.2 (2.5)		2.3		0.1
I_i[d]			46.2	50.4		91.5	85.2	3.5	1.9
$7\ 6^{+}$	45.17	47.0 (6.0)	~9.7			~0.1			

[a] Calculated energies (tab. 1) are shifted down toward the negative energies by 1.9 eV for comparison with the experimental data
[b] Energies from the spectral decomposition. FWHMs [eV] are given in parentheses
[c] Upper filled MO $14\ 8^-$ (2 electrons), filling number for the $n\ 6^{\pm}$ and $n\ 7^{\pm}$ MOs is 2, and for the $n\ 8^{\pm}$ – is 4 electrons
[d] Total intensities and the U6p electronic state densities

experimental one 1.03 [13]. However, associating the OVMO intensity only with the $U6d^27s^25f^2$ and $2O2p^4$ electrons, and the IVMO intensity – with $U6p^6$ and $2O2s^2$ electrons, one can get the theoretical ratio of 0.87, which is somewhat lower than the corresponding experimental value [13]. These results within the measurement error, at least, do not contradict the suggestion of the direct participation of the U5f electrons in the chemical bond, and the relativistic calculation results reflect correctly the partial U5f electronic density (tab. 1). These data show that about one U5f electron participates directly in the chemical bond formation and the vacant U5f states are located near the absorption edge.

In the IVMO XPS range the good agreement was reached only for the $9\ 8^-$, $8\ 8^-$ and $7\ 6^-$ orbitals characterizing the spectral width. Taking into account the comparability of the theoretical data and experimental total relative intensity, one can suggest that the calculated energies of the $4\ 7^- - 8\ 6^+$ IVMO differ significantly from the corresponding experimental data (tabs. 1 and 2).

Taking into account the relativistic calculations for the $UO_8^{12-}(O_h)$ cluster and experimental data on the core-valence levels binding energy differences for uranium [1], in the MO LCAO (molecular orbitals as linear combinations of atomic orbitals) an approximation of a schematic diagram of molecular orbitals can be built (fig. 2). This diagram enabled the understanding of the real XPS structure of uranium dioxide. In this approximation one can separate formally the antibonding $9\ 8^-(5)$, $8\ 6^-(6)$ and corresponding bonding $8\ 8^-(8)$, $7\ 6^-(9)$ IVMOs, as well as the quasiatomic (in a certain approximation) $4\ 7^-$, $5\ 7^+(6)$, $8\gamma_8^+$, $8\ 6^+(7)$, $7\ 6^-$ IVMOs attributed generally to the O2s – $U6p_{1/2}$ electrons. These experimental data show that the binding energies of quasiatomic IVMOs formed mostly from the O2s AOs have to be of the same order of magnitude. The binding energy must be around 22.5 eV, since E_O = 508 eV and for UO_2 $E_b(O1s)$ = = 530.5 eV (fig. 2). These data only partially agree with the theoretical results. Taking into account that E_U = 360.6 eV and E_1 = 362.9 eV,

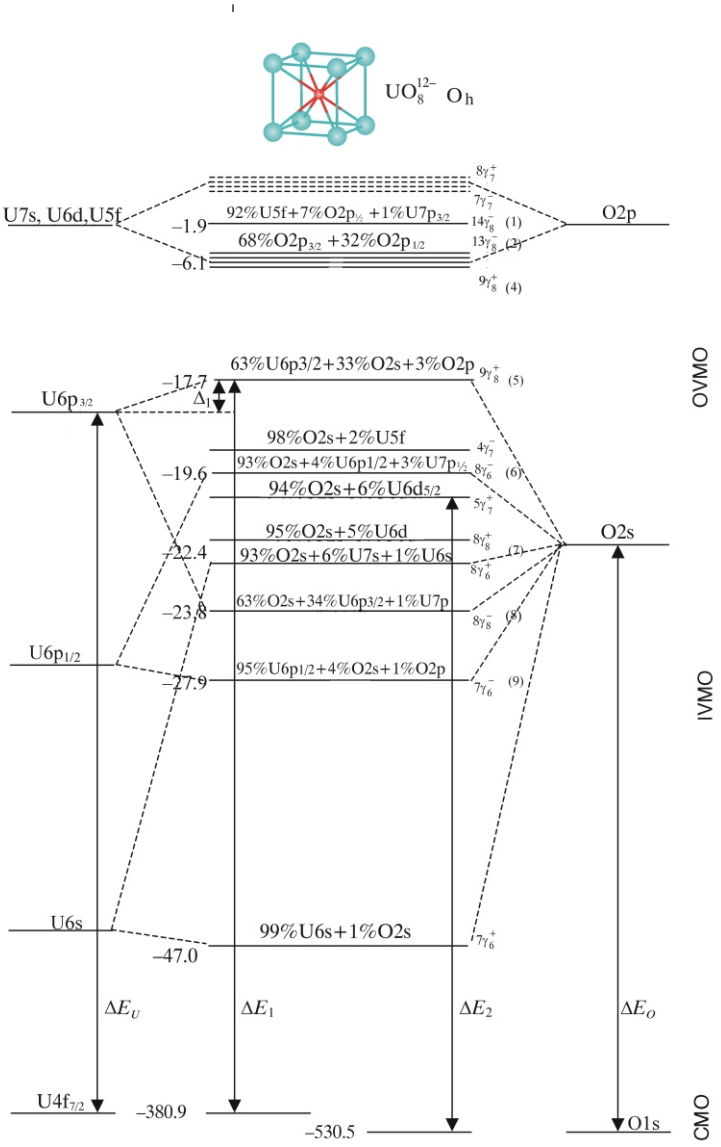

Figure 2. MO schematic diagram for the UO_8^{12-} (O_h) cluster built taking into account the theoretical and experimental data. The chemical shift during the cluster formation is not shown. The arrows indicate some experimentally measurable binding energy differences. The experimental binding energies [eV] are given to the left side. For clarity, energy levels do not reflect real energy scale

one can find $_1$ = 2.3 eV [3]. Since the binding energy difference for the 7 $_6^-$(9) and 9 $_8^-$(5) IVMO is 10.2 eV, and the U6p atomic spin-orbit splitting is E_{so}(U6p) = 10.0 eV [3], one can evaluate that perturbation is $_1$ = 0.2 eV which is lower than the corresponding value of 2.3 eV found from the core–IVMO binding energy difference. This distinction, apparently, can be attributed to the IVMO formation and this comparison can not be quite correct. The 8 $_8^-$(8) and 7 $_6^-$(9) IVMO lines are somewhat narrower than the corresponding antibonding 8 $_6^-$(6) and 9 $_8^-$ ones, which can be explained by a partial loss of the antibonding nature of these MOs due to the impurities of 3% of the O2p and 3% of the U7p AOs, respectively (tabs. 1 and 2, fig. 2, see also [3]. Figure 3a gives the expected XPS drawn on the basis of theoretical and experimental data. This spectrum has to be taken into account for more correct calculations of the electronic structure of UO_2.

Conversion electron spectroscopy (CES). One of the experimental confirmations for IVMO formation in UO_2 is the high resolution conversion electron spectral structure [14]. The qualitative identification of the CES was done on the basis of the XPS parameters using the OVMO and IVMO concept [3, 6]. As a result, it became obvious that the CES parameters can also be a quantitative measure for the correctness of theoretical calculation (figs. 1, 3b).

The total conversion transition of the E3 – multipole for the ^{235m}U nucleus ($T_{1/2}$ = 26.3 ± 0.2 min. for UO_3) from the first excited state (spin $I_1 = 1/2^+, E_1 = 76.5 \pm 0.4$ eV) to the ground nucleus state (spin $I_0 = 7/2^-, E_0 = 0$ eV) is accompanied by low energy electron photoemission. The conversion process is energetically permitted for the $U6s^26p^65f^36d^17s^27p^0$ electrons, whose shell can participate effectively in the OVMO and IVMO formation in uranium compounds.

For comparison with the experimental CES spectrum, we developed the corresponding theoret-

ical one which is based on relativistic calculations and relative one-electron partial conversion probabilities (tabs. 1 and 2, fig. 1, [15]). Since the U6p conversion cross-section is much higher than that for the other electronic shells, the CES spectrum from UO_2 reflects rather the U6p partial electronic density, and the $U6p_{1/2}$ cross-section is about 2.1 times higher than the $Up_{3/2}$ one. With this in mind, one can note a satisfactory qualitative agreement between the XPS and CES data (fig. 1). Comparison of the XPS and CES data gives three important conclusions: 1) the U6p shell participates effectively in the IVMO formation, 2) the U6p shell participates significantly in the OVMO formation, and 3) the U5f electrons from the $14\ _8^-(1)$ OVMO and electrons from the quasiatomic $4\ _7^-(6)$, $5\ _7^+(6)$, $8\ _8^+(7)$, $8\ _6^+(7)$ IVMOs, as expected, practically are not observed at 19.6 and 22.4 eV, and the $9\ _8^-(5)$, $8\ _8^-(8)$, $7\ _6^-(9)$. IVMO energies slightly differ from the corresponding theoretical values and to a greater extent agree with the experimental XPS parameters (figs. 1 and 2).

The identification of the XPS and CES structures is given in tab. 2 and fig. 3. Taking into account conversion cross-sections and intensities, the partial $U6p_{3/2,1/2}$ electronic density in UO_2 was evaluated (tab. 2). As a result, the OVMOs were found to include 0.6 U6p electrons (tab. 2), which agree better with the theoretical result for 0.2 e^-. In this case, mainly $U6p_{3/2}$ electrons participate in the chemical bond. For the IVMO region an agreement was also reached in some cases. Figure 3b gives the spectrum drawn on the basis of the theoretical and experimental data. This spectrum has to be taken into account for more correct calculations of the electronic structure of UO_2.

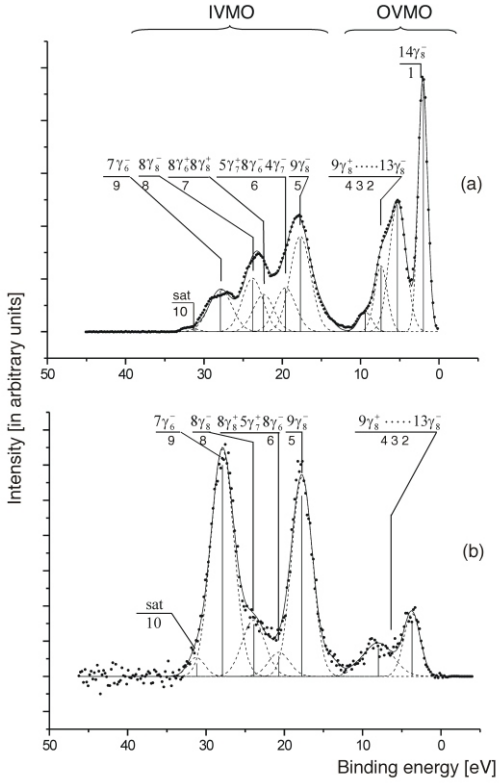

Figure 3. XPS (a) and CES (b) from UO_2 with subtracted background. The corresponding expected spectra obtained on the basis of the theoretical and experimental data are given bellow the experimental spectra as vertical bars. The spectral intensities are given in arbitrary units, the theoretical intensities are normalized in %

We would like to note that, despite approximation imperfections, the calculation results for the $UO_8^{12-}(O_h)$ cluster reflecting uranium close environment in UO_2 are in good agreement with the experimental data. It allowed for the first time a reliable interpretation of the peaks of at least the IVMO ceiling and bottom. These results can be also used for the interpretation of other X-ray spectra (Auger-, emission, absorption) of UO_2.

X-ray $O_{4,5}$(U) emission spectroscopy (XES). X-ray $O_{4,5}$(U) emission spectra reflecting the $U5d_{5/2,3/2}$ $U6p_{3/2,1/2}$,np,5f [$O_{4,5}$(U) $P_{2,3}$,O_6(U)] electronic transitions were observed in the photon energy range $60 < h\nu < 120$ eV. Its structure was distorted in the higher energy region due to the interference with absorption spectrum (fig. 4). Earlier [16], the low energy structure was associated with the ternary electronic transitions involving the core uranium shells $U5d_{5/2,3/2}$ $U6p_{3/2,1/2}$ (fig. 4, tab. 3). However, by ignoring the participation of $U6p_{3/2,1/2}$ electrons in the IVMO formation one can not properly identify fine spectral structures in X-ray $O_{4,5}$(U) emission spectra.

In our previous publication on the interpretation of fine structure interpretation [8] we took into account the fact that the U6p shell is not core shell and participates effectively in the IVMO formation. The low energy band in the $O_{4,5}$(U) XES from UO_2 is wide and poorly resolved despite a relatively high resolution of the spectrometer in the energy range 70-80 eV (fig. 4, tab. 3). It can be partially explained by an extra electronic transitions not included in tab. 3. Alternative explanation can be the formation of the higher uranium oxidation state oxides on the sample surface (the vacuum was $0.67\ 10^{-4}$ Pa), which can significantly contribute to the emission at 1 kV.

As the voltage on the X-ray tube increases to 3 kV, the contribution to the emission from the sample bulk (*i. e.* UO_2) grows and the spectrum changes. Thus, the peaks in the low energy range at 73.5, 76.2, and 79.6 eV, a small shoulder at 85,1 eV and two peaks at 95.8 and 104.7 eV become narrower, while the peak at 91.4 eV diminishes. Also, the surface decomposition in this case can not be excluded. Taking all this into account one can attribute peaks at 91.4 and 98.4 eV to the electronic transitions from the outer valence band to the $U5d_{5/2,3/2}$ shells, and those at 95.8 and 104.7 eV to the transitions

Table 3. X-ray $O_{4,5}$(U) emission ($U5d_{5/2,3/2}$ U6p,5f,np) transitions [eV] in metallic U and UO_2 on the basis of XPS and XES

U				UO_2			
N	Transitions	XPS	XES	N	Transitions	XPS	XES
				1	$U5d_{5/2}$ 8 $_8^-$	73.5	73.5
1*	$U5d_{3/2}$ $U6p_{1/2}$	76.0		2	$U5d_{3/2}$ 7 $_6^-$	77.6	76.2
							78.0
2*	$U5d_{5/2}$ $U6p_{3/2}$	77.4		3	$U5d_{5/2}$ 9 $_8^-$	79.6	79.6
				4	$U5d_{3/2}$ 8 $_8^-$	81.7	83.3
				5	$U5d_{3/2}$ 8 $_6^-$	85.9	85.1
3*	$U5d_{3/2}$ $U6p_{3/2}$	86.0		6	$U5d_{3/2}$ 9 $_8^-$	87.8	87.4
				7	$U5d_{5/2}$ OVMO	91.2	91.4
4*	$U5d_{5/2}$ $U5f_{7/2,5/2}$	95.4*		8	$U5d_{5/2}$ $5f_{5/2}$	95.4	95.8
				9	$U5d_{3/2}$ OVMO	99.4	98.4
5*	$U5d_{3/2}$ $U5f_{5/2}$	104.0*		10	$U5d_{3/2}$ $5f_{5/2}$	103.6	104.7
				11			109.2

* Values obtained on the basis of the experimental evaluation taking into account the experimental $U5d_{5/2,3/2}$-U5f binding energy differences for $UO_{2,06}$

U5f $U5d_{5/2,3/2}$. It has to be noted that the XPS and XES data are in good qualitative agreement (fig. 4, tab. 3).

In the low energy transition energy range involving the bonding MOs ($U5d_{5/2}$ 8 $_8^-$) at 73.5 eV for UO_2 calculated on the basis of the XPS data no narrow peaks were observed (fig. 4), while the peaks reflecting the transitions from the corresponding antibonding MOs ($U5d_{5/2}$ 8 $_8^-$ and $5d_{3/2}$ 8 $_8^-$) can be distinguished despite of their low intensity. Calculations show that if the antibonding 9 $_8^-$ orbital consists of 63% of U6p states, the corresponding bonding 8 $_8^-$ one is 34% (fig. 2). Therefore, the transitions $U5d_{5/2}$ 8 $_8^-$ in UO_2 can hardly be separated from the wide band due to its low intensity. However, this consideration can be done only in the approximation that the MOs keep a partial AO nature. Also, during the XES formation an initial state with a hole on the U5d level transits into the final state with a hole on one of the MOs, while during the XPS formation the initial state does not have any holes and the final one has a hole on one of the core or valence level. This difference can lead to a significant difference in the structures of the considered spectra, and the compariso of the XPS and XES is approximate. The more strict comparison requires precise theoretical calculations for the emission spectra.

The obtained data show that the $O_{4,5}$(U) XES structure of UO_2 can be identified only taking into account the effective IVMO formation from, in particular, the relatively deep U6p and O2s AOs. These results are another experimental confirmation of the effective IVMO formation in UO_2.

X-ray near $O_{4,5}$(U) edge absorption spectroscopy (XAS). The X-ray near $O_{4,5}$(U) edge (near the U5d) absorption spectrum in the excitation energy range 90-120 eV exhibits an unusual structure for X-ray absorption spectra from solid materials. This structure consists of the two resonant bands of different widths and intensities. The total electron and total quantum yield spectra from uranium oxides has been shown to be similar by shape, energy position, and width; the only difference was in the intensity ratio [17]. Since the absorption edge of the low intensity peak is 97.5 eV, which is close to the $U5d_{5/2}$ binding energy for UO_2 (97.3 eV), this peak was attributed to the $U5d_{5/2}$ U5f transition (fig. 5). In this case the $U5d_{3/2}$ U5f absorption peak is supposed to be at about 8 eV higher since $U5d_{3/2}$ binding energy is 105.5 eV [10] and lower intensity is due to the lower $U5d_{3/2}$ population and the selection rule (the total quantum number $j = 3/2$ is less than $j = 5/2$). This explains the shoulder at 107 eV in the quantum yield spectrum from UO_2. The work [18] considers in the ionic approximation for U^{4+} the transition $U5f^2(^3H_4)$ $U5d^95f^3(^3G_3, ^3H_4, ^3I_5)$ and finds out that the low energy peak reflects generally the $U5d_{5/2}$ $U5f^3$ transitions, and a shoulder at 107 eV is due to the $U5d_{3/2}$ $U5f^3$ transitions. The main intensity of the higher energy peak was attributed to the U5d U7p,8p and 6f transitions. For the qualitative

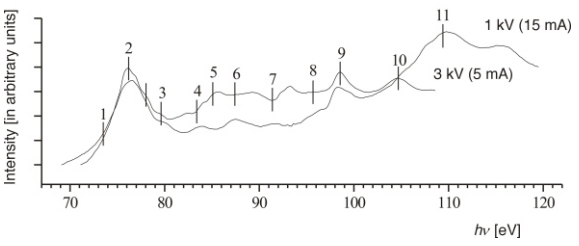

Figure 4. X-ray $O_{4,5}$(U) emission spectra reflecting the U5d U6p,5f,np transitions in UO_2 measured at 1 and 3 kV

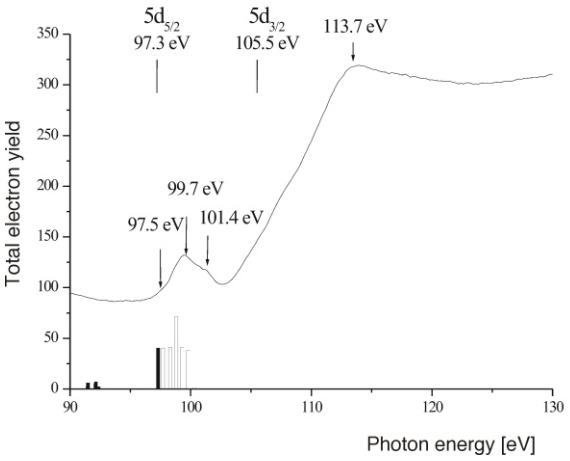

Figure 5. Total electron yield from UO_2. The $U5d_{5/2,3/2}$ binding energies are given above the spectrum. The density of the U5f occupied (full) and vacant (hollow) states is shown bellow the spectrum as vertical bars

comparison fig. 5 gives the results of the theoretical calculations of the density of the vacant and filled U5f electronic states for the $UO_8^{10-}(O_h)$ cluster reflecting uranium close environment in UO_2. For comparison the theoretical spectrum was shifted by 1.9 eV (the U5f binding energy in UO_2) to the right. This comparison shows that the low energy peak, apparently, must be attributed to the U5f vacant states. It has to be noted that right after these states (to the right by the energy scale on fig. 5) the vacant U7p states are located, and the transitions U5d U7p can take place. These data at least do not contradict the suggestion of direct participation of the U5f electrons in the chemical bond. Indeed, attributing the XAS structure of UO_2 at 100 eV (fig. 5) to the antibonding MOs, one can see that the corresponding bonding OVMO states have to be filled with the U5f electrons.

Resonant X-ray photoelectron spectroscopy (RXPS). The paper [10] considers the electron photoemission under the excitation $h\nu$ around the $O_{4,5}$(U) edge from UO_2 formed on the surface of uranium foil (fig. 6). The resonance was expected to appear at the excitation energies 100-113 eV (see fig. 5). Indeed, the more intense peaks appear in the spectrum excited at $h\nu$ = 110 eV (fig. 6). If earlier [19] only the OVMO (0-13 eV BE) intensity change was observed, the authors of [10] for the first time observed the resonance in UO_2 and ThO_2 for the OVMO and IVMO electrons in the binding energy range 0-40 eV (fig. 6). In this case to a first approximation this structure for the actinide (An) compounds can be described by the following excitation and decay processes:

$$An5d^{10}(IVMO)^k(OVMO)^m\,5f^n \quad h\nu$$

$$An5d^{9}(IVMO)^k(OVMO)^m\,5f^{n\ 1} \qquad (1)$$

$$An5d^{9}(IVMO)^k(OVMO)^m\,5f^{n\ 1} \quad (e^2/r)$$

$$An5d^{10}(IVMO)^k(OVMO)^m\,5f^{n\ 1} \quad e \qquad (2)$$

$$An5d^{9}(IVMO)^k(OVMO)^m\,5f^{n\ 1} \quad (e^2/r)$$

$$An5d^{10}(IVMO)^k(OVMO)^{m\ 1}5f^n \quad e \qquad (3)$$

$$An5d^{9}(IVMO)^k(OVMO)^m5f^{n\ 1} \quad (e^2/r)$$

$$An5d^{10}(IVMO)^{k\ 1}(OVMO)^m5f^n \quad e \qquad (4)$$

It has to be noted that together with this process a regular photoemission takes place. Since the considered resonant spectra are mostly due to the Auger electrons rather than to the photoemission, they reflect mostly the An*np* and An*5f* partial state densities. The observed washout of the structure in the ~15-40 eV energy range was explained by the IVMO formation. Since during the resonance the

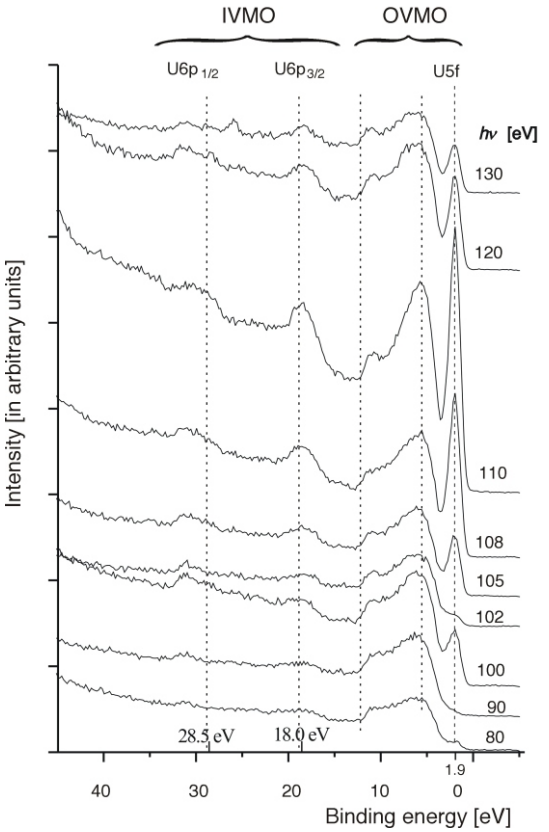

Figure 6. RXPS from UO_2 formed on the metallic uranium foil collected at different SR excitation energies. Numbers show energies of $h\nu$ in eV. Intensities are normalized to the current of SR beam. The binding energies for UO_2 are given bellow the spectra. The C1s binding energy from the absorbed hydrocarbons on the sample surface was accepted to be 285.0 eV

largest intensity changes are expected for the U5f,6p related peaks, the obtained data allows three important conclusions. First – the peak at 1.9 eV is attributed to the localized U5f electrons. Second – the U5f electrons participating directly in the chemical bond are delocalized which results in the increase of OVMO intensity. Third – the U6p electrons participate effectively in the IVMO and probably OVMO formation, which results in the intense resonant structure in the IVMO energy range. This structure reflects the partial U6p electronic density in this spectral region.

Resonant X-ray $O_{4,5}$(U) emission spectroscopy (RXES). The RXES from UO_2 collected at excitation energies 104.4, 107.2, 113.8, and 120 eV [9] are shown on fig. 7. The RXES structure depends strongly on the near resonance excitation energy. The fixed energy non resonant XES (fig. 7) is given bellow the spectra for comparison (see fig. 4). One can see a satisfactory agreement between the resonant and non-resonant spectra. Thus, the peaks A and B separated by about 8 eV are attributed to the transitions $U5d_{5/2,3/2}$ OVMO. They are observed in both resonant and non-resonant spectra. Figure 7 shows that peak B is more intense in the RXES from UO_2. It indicates that the transition $U5d_{3/2}$ OVMO prevails over the $U5d_{5/2}$ OVMO one. The peak A grows in the non-resonant spectra. It has to be noted that the filled U6p states present in the OVMO (0.6 e^- of the U6p electrons in UO_2, see tab. 2) and the transition from the MOs containing the U6p electrons also should appear in the considered spectra. Indeed, peak B is obviously structured.

The RXES from UO_2 and UO_3 collected at 101 eV excitation energy show a significant difference (fig. 8). Unlike the UO_3 one, the UO_2 RXES

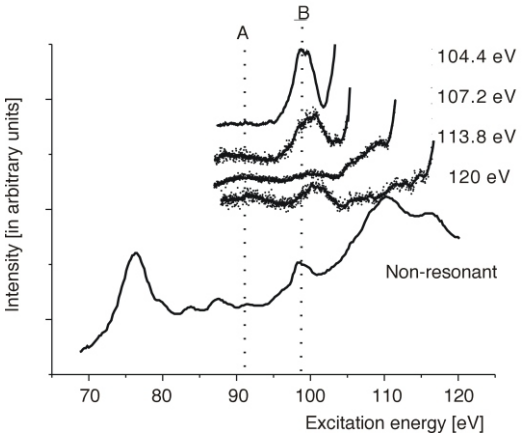

Figure 7. Resonant X-ray $O_{4,5}$(U) emission spectra from UO_2 collected at different SR excitation energies $h\nu$ [eV]. Corresponding non-resonant spectrum is given below for comparison (see fig. 4)

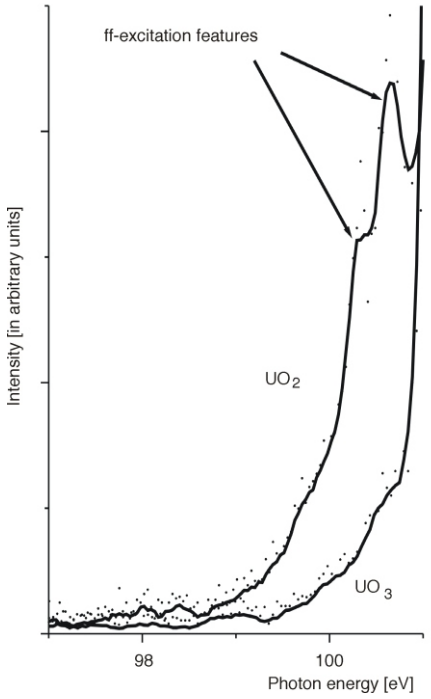

Figure 8. Resonant X-ray $O_{4,5}$(U) emission spectra from UO_2 and UO_3 collected at the excitation SR energy $h\nu$ = 101 eV. The spectrum from UO_2 exhibits the structure reflecting the ff-excitation process

shows the two peaks attributed to the ff-excitation [9]. The ff-excitation is expected to appear with a higher probability in the spectra of compounds with the more ionic type of bond, like UO_2. A more reliable interpretation of the ff-excitation process requires more correct calculations of the RXES structure taking into account the many-body perturbation and the charge transfer effect.

The observed RXES transitions agree with the suggestion that the filled U5f and probably U6p

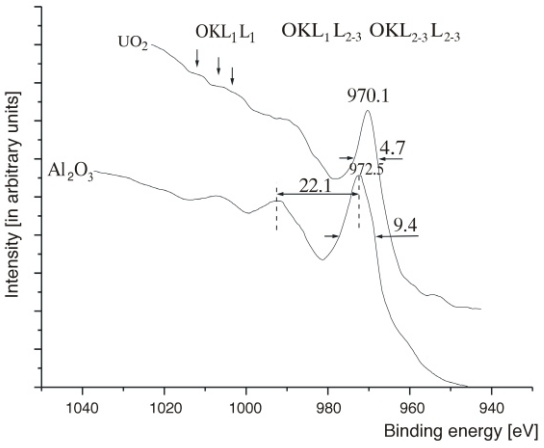

Figure 9. Auger OKLL spectra from Al_2O_3 and UO_2 collected at the AlK $_{1,2}$ (1486.6 eV) excitation energy

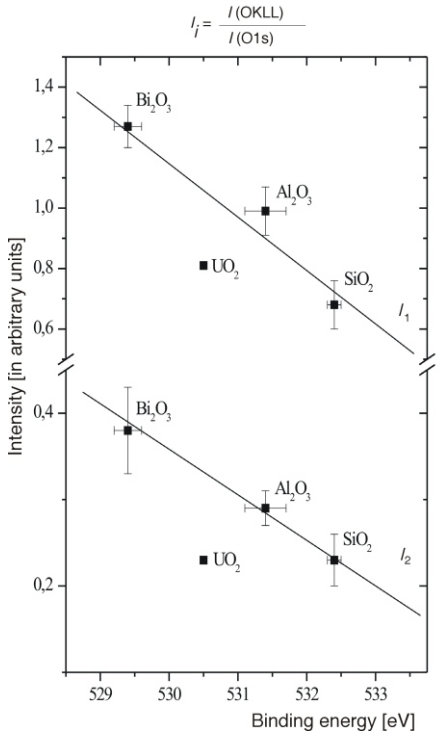

Figure 10. Dependence of the relative Auger $OKL_{2-3}L_{2-3}$ and OKL_1L_{2-3} intensities on the O1s binding energies for: Bi_2O_3, Al_2O_3, SiO_2, and UO_2

states are present in the outer valence band. This agrees with the data of other considered methods.

Auger OKLL spectroscopy of oxygen. Auger OKLL spectrum from, for example Al_2O_3, where the IVMOs do not form effectively, consists of the three well observed structured lines reflecting the $OKL_{2-3}L_{2-3}$ (O1s O2p), OKL_1L_{2-3} (O1s O2s,2p), OKL_1L_1 (O1s O2s) transitions (fig. 9). In previous work [20], we have established a quantitative correlation of the relative Auger intensity, characterizing the partial density of the filled oxygen electronic states, on the O1s XPS binding energy, characterizing the total density of the valence electronic states on the oxygen ion (fig. 10). The relative Auger intensities are given as area ratios OKLL/O1s. The Auger OKLL spectrum of UO_2 differs significantly from the corresponding spectrum of Al_2O_3, SiO_2, and Bi_2O_3 (figs. 9, 10 and tab. 4). The $OKL_{2-3}L_{2-3}$ FWHM for UO_2 is significantly lower (< 5 eV) than the corresponding FWHMs for other oxides. It can be explained by the fact that the partial O2p density OVMO band for UO_2 is significantly narrower than that for other studied oxides (fig. 9). The OKL_1L_{2-3} and OKL_1L_1 Auger regions for UO_2 exhibit more complicated structures than those for the other studied oxides. It can be explained by the IVMO formation from the U6p - O2s interaction. The relative decrease of intensity of the $OKL_{2-3}L_{2-3}$ and OKL_1L_{2-3} Auger lines for UO_2 when compared to the other studied oxides (fig. 10) apparently can also be attributed to the IVMO formation.

Table 4. The O1s binding energies E_b [eV] and relative Auger $OKL_{2-3}L_{2-3}$ and OKL_1L_{2-3} intensities I[(a)] [rel. units] for oxides: Bi_2O_3, Al_2O_3, SiO_2, and UO_2

N	Oxides	E_b	I_1	I_2
1	Bi_2O_3	529.4 0.2	1.27 0.07	0.38 0.05
2	Al_2O_3	531.4 0.3	0.99 0.08	0.29 0.02
3	SiO_2	532.4 0.1	0.68 0.08	0.23 0.03
4	UO_2	530.5	0.81	0.23

[(a)] Relative intensities were taken as spectral area ratios (Auger OKLL)/(XPS O1s) measured during the same experiment

The results of the simultaneous registration of the Auger OKLL and XPS O1s,2s,2p spectra of UO_2 and other oxides in the binding energy range 0-540 eV allowed a qualitative evaluation of the relative valence electronic oxygen state density in UO_2 and an experimental confirmation for the IVMO formation in this oxide.

We would like to note that a similar complex study was done also for other actinide compounds, these results are partially reflected in [3].

CONCLUSIONS

(1) Using UO_2 as an example we analyzed new data on the chemical bond nature obtained by the X-ray photoelectron, conversion electron, non-resonant and resonant X-ray $O_{4,5}(U)$ emission, near $O_{4,5}(U)$ edge absorption, resonant photoelectron and Auger OKLL spectroscopy taking into account the data of the relativistic electronic structure calculations for the $UO_8^{12-}(O_h)$ cluster reflecting uranium close environment in UO_2.

(2) Despite the traditional opinion that before the chemical bond formation the An5f- electrons get promoted to, for example, the An6d atomic orbitals, the theoretical calculations show and experimental data confirm that the An5f atomic shells (~1 U5f electron) can participate directly in the formation of molecular orbitals in actinide compounds. About 2 U5f electrons weakly participating in the chemical bond are localized at –1.9 eV, ~1 U5f participating in the chemical bond is delocalized in the OVMO binding energy range from –4 to –9 eV, and the vacant U5f electronic states are generally delocalized in the low positive energy range (0-5 eV).

(3) The U6p electrons (0.6 U6p electrons) were experimentally shown to participate significantly in the OVMO formation beside the IVMO formation, which agrees with the theoretical data.

(4) It was established that, for example, the bonding 8 $_8^-$(8) and corresponding antibonding 9 $_8^-$(5) IVMO are formed generally from the $U6p_{3/2}$ and O2s AOs and their calculated compositions (63% of $U6p_{3/2}$ and 33% of O2s and 34% of $U6p_{3/2}$ and 63% of O2s AOs) differ slightly from

the experimental data (75% of U6$p_{3/2}$ and 21% of O2s and 22% of U6$p_{3/2}$ and 75% of O2s AOs). Electrons from these orbitals in the aggregate were suggested to strengthen the chemical bond in uranium dioxide.

(5) The relativistic calculations confirm an earlier suggestion made on the basis of the non-relativistic calculations that the filled U6$p_{3/2}$ and O2s AOs participate mostly in the IVMO formation, while the U6$p_{1/2}$ component participates to a lesser extent.

ACKNOWLEDGEMENT

This work was supported by the RFBR grants 04-03-32892 and 02-03-32693

REFERENCES

[1] Teterin, Yu. A., Gagarin, S. G., Inner Valence Molecular Orbitals of Compounds and the Structure of X-Ray Photoelectron Spectra, *Russian Chemical Reviews, 65* (1996), 10, pp. 825-847

[2] Teterin, Yu. A., Teterin, A. Yu., The Structure of X-Ray Photoelectron Spectra of Lanthanide Compounds, *Russian Chemical Reviews, 71* (2002), 5, pp. 403-441

[3] Teterin, Yu. A., Teterin, A. Yu., The Structure of X-Ray Photoelectron Spectra of Light Actinides, *Russian Chemical Reviews, 73* (2004), 6, pp. 588-631

[4] Teterin, Yu. A., Ryzhkov, M. V., Teterin, A. Yu., Panov, A. D., Nikitin, A. S, Ivanov, K. E., Utkin, I. O., The Nature of Chemical Bond in Trioxide -UO_3, *Nuclear Technology & Radiation Protection, 17* (2002), 1-2, pp. 3-12

[5] Teterin, Yu. A., Teterin, A.Yu., Yakovlev, N. G., Utkin, I. O., Ivanov, K. E., Shustov, L. D., Vukchevich, L., Bek-Uzarov, G. N., X-Ray Photoelectron Study of Actinide (Th, U, Pu, Am) Nitrates, *Nuclear Technology & Radiation Protection, 18* (2003), 2, pp. 31-35

[6] Teterin, Yu. A., Kulakov, V. M., Baev, A. S., Nevzorov, N. B., Melnikov, I. V., Streltsov, V. A., Mashirov, L. G., Suglobov, D. N., Zelenkov, A.G., A Study of Synthetic and Natural Uranium Oxides by X-Ray Photoelectron Spectroscopy, *Phys. Chem. Minerals, 7* (1981), pp. 151-158

[7] Grechuhin, D. P., Zhudov, V. I., Zelenkov, A. G., Kulakov, V. M., Odinov, B.V., Soldatov, A. A, Teterin, Yu. A., Direct Observation of the Strong Hybridization of Electronic Orbits in the Spectra of the Inner Conversion Electrons, *Pisma v ZhETF, 31* (1980), 11, pp. 627-630

[8] Teterin, Yu. A., Terechov, V. A., Teterin, A. Yu., Ivanov, K. E., Utkin, I. O., Lebedev, A. M., Vukchevich, L., Inner Valence Molecular Orbitals and Structyre of X-Ray $O_{4,5}$ (Th, U) Emission Spectra in Thorium and Uranium Oxides, *J. Electron Spectrosc. Relat. Phenom., 96* (1998), pp. 229-236

[9] Ivanov, K. E., Teterin, Yu. A., Shuh, D. K., Teterin, A. Yu., Butorin, S. M., Guo, J.-H., Magnuson, M., Nordgren, J., The Structure of Resonant X-Ray $O_{4,5}$(U)- Emission Spectra of Urnium Oxides UO_2 and -UO_3, *Proceedings*, 4th International Yugoslav Nuclear Society Conference (YUNSC- 2002), Belgrade, Yugoslavia, September 30 – October 4, 2002, VINČA Institute of Nuclear Sciences, Yugoslav Nuclear Society, Belgrade, 2003, pp. 431-434

[10] Teterin, Yu. A., Utkin, I. O., Teterin, A. Yu., Reich, T., Hillebrecht, F. U., Molodtsov, S. L., Varykhalov, A. Yu., Gudat, W., BESSY GmbH, 12489, Berlin, Germany, Annual Report, 2004

[11] Ryzhkov, M. V., Gubanov, V. A., Teterin, Yu. A., Baev, A. S., Electronic Structure and X-Ray Photoelectron Spectra of Uranyl Compounds (in Russian), *Radiohimiya, 1* (1991), pp. 22-28

[12] Band, I. M., Kharitonov, Yu. I., Trzhaskovskaya, M. B., Photoionization Cross Sections and Photoelectron Angular Distributions for X-Ray Line Energies in the Range 0.132-4.509 keV. Targets: 1 Z 100, *Atomic Data and Nuclear Data Tables, 23* (1979), pp. 443-505

[13] Teterin, Yu. A., The An5f-States of Actinides (Th, U, Np, Pu, Am, Cm, Bk) in Compounds and Parameters of Their X-Ray Photoelectron Spectra (in Russian), *Kondensirovannye Sredy I Mezhfaznye Granitsy, 2* (2000), 1, pp. 60-66

[14] Panov, A. D., Zhudov, V. I., Teterin, Yu. A., Conversion Spectra of Electrons of Valence Shells of Oxygen-Containing Uranioum Compounds, *J. Structural Chem., 39* (1998), 6, pp. 1047-1051

[15] Grechuhin, D. P., Soldatov, A. A., Isomer ^{235}U (73 eV; $½^+$); Excitation During Interaction with Electrons (in Russian), *Yadernaya Fizika, 28, 5,11* (1978), pp. 1206-1222

[16] Lyahovskaya, I. I., Ipatov, V. M., Zimkina, T. M., Long-Wave X-Ray 5d Spectra of Thorium and Uranium in Compounds with Oxygen and Fluorine, *J. Structural Chem., 18* (1977), 4, p.668-672

[17] Zimkina, T. M., Lyahovskaya, I. I., Shulakov, A. S., Atomic Resonance in the 5d Absorption (in Russian), Reflection and Radiation Spectra of Thorium and Uranium in Compounds, *Optika I Spektroskopiya, 62* (1987), 2, pp. 285-288

[18] Imoto, S., Miyake, C., Adachi, H., Hinatsu, Y., Taniguchi, K., Fujima, K., Abstacts of Reports on Actinides – 1981, September 10-15, 1981, LBL and LLNL Berkeley, California, pp. 99-101

[19] Cox, L., Ellis, W. P., Cowan, R., Allen, J. W., Oh, S.-J., Lindau, I., Pate, B. B., Arko, A. J., Valence Photoemission in UO_2(111) Near the 5d Resonant Photon Energy, *Phys. Rev. B., 35* (1987), 11, pp. 5761-5765

[20] Teterin, Yu. A., Ivanov, K. E., Teterin, A. Yu., Lebedev, A. M., Utkin, I. O., Vukchevich, L., Auger and X-Ray Photoelectron Spectroscopy Study of the Density of Oxygen States in Bismuth, Aluminum, Silicon and Uranium Oxides, *J. Electron Spectrosc. Relat. Phenom., 101-103* (1999), pp. 401-405

Јурij А. ТЕТЕРИН, Антон Ј. ТЕТЕРИН

ПРОУЧАВАЊЕ ЕЛЕКТРОНСКИХ СТРУКТУРА АКТИНИДА САВРЕМЕНИМ РЕНДГЕНСКИМ СПЕКТРАЛНИМ МЕТОДАМА – ПРИМЕР УРАНИЈУМОКСИДА UO_2

Фина спектрална структура рендгенског фотоелектрона уранијумдиоксида UO_2 у области енергије везе од 0-~40 eV, углавном је повезана са електронима спољашњих (0-15 eV) и унутрашњих (15-40 eV) валентних молекулских орбитала образованих од некомплетно попуњених U5f,6d,7s и O2p љуски и комплетно попуњених U6p и O2s љуски суседних уранијумових и кисеоникових јона. Ово је у сагласности са резултатима релативистичких прорачуна електронске структуре $UO_8^{12-}(O_h)$ кластера који одражава уранијумову непосредну околину у UO_2, а што је потврђено подацима рендгенске спектроскопије (конверзијом електрона, нерезонантном и резонантном, $O_{4,5}$(U) емисијом, $O_{4,5}$(U) апсорпцијом у близини границе, резонантним фотоелектроном Ожеовским електроном). Успостављена је фина спектрална структура рендгенског фотоелектрона повезана са спољашним и унутрашњим валентним молекулским орбиталама која води закључку о степену учешћа U6p,5f електрона у хемијској вези, о структури уранијумовог непосредног окружења и међуатомским растојањима у оксидима. Укупан допринос електрона са унутрашњих валентних молекулских орбитала апсолутној вредности хемијске везе може се упоредити са доприносом оних са спољашњих орбитала. Мора се запазити да унутрашње валентне молекулске орбитале доприносе једињењима маког елемента из периодног система. Ово је нова научна чињеница у хемији и физици чврстог стања.